

A Tutorial on Data-Driven Eigenvalue Identification: Prony Analysis, Matrix Pencil and Eigensystem Realization Algorithm

Anas Almunif, Lingling Fan^{*†}, and Zhixin Miao

Department of Electrical Engineering, University of South Florida, Tampa, FL 33620, USA

Abstract

To identify power system eigenvalues from measurement data, Prony analysis, Matrix Pencil (MP), and Eigensystem Realization Algorithm (ERA) are three major methods. This paper reviews the three methods and sheds insight on the principles of the three methods: eigenvalue identification through various Hankel matrix formulations. In addition, multiple channel data handling and noise resilience techniques are investigated. In the literature, singular value decomposition (SVD)-based rank reduction technique has been applied to MP and resulted in a reduced-order system eigenvalue estimation and an excellent noise resilient feature. In this paper, ERA is refined using the SVD-based rank reduction to achieve superior performance. Further, a reduced-order Prony analysis method is proposed. With this technique, Prony analysis can not only give reduced-order system eigenvalues, but also become noise resilient. Four case studies are conducted to demonstrate the effectiveness of the eigenvalue identification methods, including a tutorial example of an RLC circuit resonance, a power grid oscillation case study for a 16-machine 68-bus system, an example of subsynchronous resonance (SSR) of a type-3 wind grid integration system, and real-world oscillation events captured by Independent System Operator-New England (ISO-NE).

Index Terms

Prony analysis; Matrix Pencil; Eigensystem Realization Algorithm; singular value decomposition; Hankel matrix; power system oscillations; subsynchronous resonances.

I. INTRODUCTION

Using measurement data, e.g., synchrophasors from Phasor Measurement Units (PMUs), to find out system dynamic information is of practical interest [1]. One example is the identification of reduced-order system models. In the literature, many of the current approaches in power system model reduction rely on the assumption that a high-order system model is known. Following this assumption, methods such as balanced truncation and Krylov, are implemented to find reduced-order models, e.g., [2], [3]. An alternative approach is to directly identify a reduced-order model based on measurements.

Identification of system eigenvalues based on measurements taken from dynamic events is a fundamental step towards a reduced-order model identification. Three methods of electromechanical oscillation damping estimation, i.e., subspace method, spectral independent component analysis, and wavelet transform, have been compared in a 2011 paper [4]. Curve fitting of frequency-domain transforms is another approach for oscillation identification, e.g., [5].

An IEEE PES taskforce report [6] on electromechanical mode identification has been published in 2012. In Chapter 1 of this report, Prony analysis, Matrix Pencil (MP), and Eigensystem Realization Algorithm (ERA) are discussed as the three major linear system identification methods for ringdown time-domain signals captured for transient events.

Prony analysis was introduced to the power system oscillation mode estimation by J. Hauer [7]. As an extension, Prony analysis based on multiple channel data was presented in [8]. In the authors' prior work [9], multiple channel Prony analysis was formulated as a weighted least squares estimation problem with the weights obtained from single-channel Prony analysis.

Using Matrix Pencil (MP) to estimate dynamic system eigenvalues for an electromagnetic transient response was presented in [10], [11]. This method was applied to power systems in 2005 to estimate dominant oscillation modes from Western Electricity Coordinating Council (WECC) frequency responses of 6 seconds [12]. In [13], MP and Prony analysis are compared for their capabilities of modal extraction of noisy power system signals. MP has been proven to be more capable of mode extraction than Prony analysis.

Eigensystem Realization Algorithm (ERA) for parameter identification and model reduction of dynamical systems was introduced in 1985 [14] relying on system realization theory introduced by Gilbert [15] and Kalman [16]. Applying ERA in power systems to find low-order models from time-domain simulation data has been investigated in [17].

All three methods form Hankel matrices from measurement data. In Prony analysis, a single Hankel matrix is formed, where eigenvalues are found by identifying the real coefficients from the polynomial characteristic equation through least square estimation (LSE). In MP and ERA, shifted Hankel matrices are formed and the relation between the two matrices are explored.

^{*}Correspondence to: Lingling Fan, Department of Electrical Engineering, University of South Florida, Tampa, FL 33620, USA

[†]E-mail: linglingfan@usf.edu

In MP, the two matrices are related with system eigenvalues and a generalized eigenvalue problem is formed [14]. In ERA, the two shifted Hankel matrices are related with system matrix A to find the eigenvalues.

While the 2012 Taskforce report offers a great guideline on the three methods, a thorough examination on their principles, multiple data handling, noise resilient techniques, and applications in large-scale power grid dynamics and power electronic converter penetrated system dynamics is of great importance. Further, data-driven modeling technique of dynamic mode decomposition (DMD) and Koopman operator, which has been developed for fluid dynamics, was recently introduced to the power systems [18]. DMD allows mode identification and coherent generator identification, and it also relies on shifted Hankel matrix construction and singular value decomposition (SVD). Hence, a tutorial on Prony analysis, MP, and ERA is deemed necessary.

The contribution of this paper is three-fold.

- First, this paper has reviewed and shed insight on the three major methods for eigenvalue identification applied in power systems and identified the key technique of noise resilience as SVD-based rank reduction. SVD-based rank reduction technique has been implemented in MP and achieved system order reduction and noise resilience [11], [19]. This technique is implemented in ERA for one of the Hankel matrices [6]. In this paper, the rank reduction technique is further implemented on the second Hankel matrix of ERA to achieve a superior performance.
- Second, Prony analysis method is improved to achieve reduced-order system eigenvalue identification and noise resilience. Prony analysis is known to be sensitive to system order assumptions. If the system order is assumed to be low, the reconstructed signal based on the identified eigenvalues poorly matches the original signal, especially for noisy signals. In this paper, two techniques are employed, namely, Hankel matrix rank reduction and eigenvalue reduction. The reduced-order Prony analysis method gives comparable performance as MP and ERA. While similar improvement has been made in [20] in 2004, the effect of Hankel matrix rank reduction on the eigenvalue distribution was not examined then. In this paper, a radical change of eigenvalue distribution is demonstrated as the effect.
- Third, this review paper extends the application scope of those methods. While almost all previous literature focuses on power grid electromechanical oscillations, this paper demonstrates that the methods can be applied to detect a wide range of dynamics, including both electromechanical dynamics and electromagnetic dynamics. Three case studies, including an RLC circuit example for electromagnetic dynamics, a large-scale power grid oscillation example for electromechanical dynamics, and a type-3 wind subsynchronous resonance (SSR) example for electromagnetic dynamics, clearly demonstrate the effectiveness of the three methods. Further, the capability of the proposed methods is validated by analyzing real-world oscillation events provided by Independent System Operator-New England (ISO-NE).

The remaining sections are organized as follows. Section II presents the principles of the three methods. Section III proceeds to the model reduction techniques used in the literature for MP and the innovation of Prony analysis improvement using Hankel matrix rank reduction technique. Section IV presents case studies. Section V concludes the paper.

II. PRINCIPLES OF THE THREE METHODS

A. Prony Analysis

Consider a Linear-Time Invariant (LTI) system with the initial state of $x(0) = x_0$, where $x \in \mathbb{R}^n$ is the stator variable column vector. The dynamic model can be expressed as the follows.

$$\dot{x}(t) = Ax(t), \quad y(t) = Cx(t) \quad (1)$$

where $y \in \mathbb{R}$ is a scalar output, $A \in \mathbb{R}^{n \times n}$ and $C \in \mathbb{R}^{1 \times n}$ are system dynamic and measurement matrices. The order of the system is n if A is full rank. Notations λ_i , p_i , and q_i represent the i -th eigenvalue, the corresponding right eigenvector, and the left eigenvector of A respectively. The scalar output y can be represented as:

$$y(t) = \sum_{i=1}^n \underbrace{C(q_i^T x_0)}_{R_i} p_i e^{\lambda_i t}, \quad (2)$$

where R_i is named as a residual.

The observed or measured $y(t)$ consists of $N + 1$ samples which are equally spaced by Δt . The samples are notated as $y_k = y(t_k)$, $k = 1, \dots, N$. k th sample y_k can be written in the exponential form as:

$$y_k = y(t_k) = \sum_{i=1}^n R_i z_i^k, \quad k = 0, \dots, N, \quad (3)$$

where $z_i = e^{\lambda_i \Delta t}$, and z_i is the i th eigenvalue of the system in discrete time domain. z_1, z_2, \dots, z_n are the roots of the n -th characteristic polynomial function of the system:

$$z^n - (a_1 z^{n-1} + a_2 z^{n-2} + \dots + a_n z^0) = 0. \quad (4)$$

While the roots may be complex numbers, the system polynomial coefficients a_i are real numbers.

From (4), the linear prediction model can be obtained.

$$z^n = a_1 z^{n-1} + a_2 z^{n-2} + \dots + a_n z^0 \quad (5)$$

$$\Rightarrow y_n = a_1 y_{n-1} + a_2 y_{n-2} + \dots + a_n y_0 \quad (6)$$

A vector of the signal samples from step n to step N can be expressed as an overdetermined problem or LSE problem (7).

$$\underbrace{\begin{bmatrix} y_n \\ y_{n+1} \\ \vdots \\ y_N \end{bmatrix}}_Y = \underbrace{\begin{bmatrix} y_{n-1} & y_{n-2} & \cdots & y_0 \\ y_n & y_{n-1} & \cdots & y_1 \\ \vdots & \vdots & \ddots & \vdots \\ y_{N-1} & y_N & \cdots & y_{N-n} \end{bmatrix}}_H \underbrace{\begin{bmatrix} a_1 \\ a_2 \\ \vdots \\ a_n \end{bmatrix}}_a \quad (7)$$

H is a Hankel matrix of $(N + 1 - n) \times n$ dimension. The best estimate of a is found from the following normal equation.

$$\hat{a} = H^\dagger Y \quad (8)$$

where H^\dagger denotes the Moore-Penrose pseudoinverse of H which is defined as: $H^\dagger = (H^T H)^{-1} H^T$, and the superscript T represents transpose. The eigenvalues of the discrete system z_i can be found by seeking the roots of the polynomial (4), while those of the continuous system λ_i can be found as $\frac{\log z_i}{\Delta t}$.

To find the residuals R_i , Equation (3) is examined. It can be expressed as another LSE, shown in (9).

$$\begin{bmatrix} z_1^0 & z_2^0 & \cdots & z_n^0 \\ z_1^1 & z_2^1 & \cdots & z_n^1 \\ \vdots & \vdots & \ddots & \vdots \\ z_1^N & z_2^N & \cdots & z_n^N \end{bmatrix} \begin{bmatrix} R_1 \\ R_2 \\ \vdots \\ R_n \end{bmatrix} = \begin{bmatrix} y_0 \\ y_1 \\ \vdots \\ y_N \end{bmatrix} \quad (9)$$

Solving (9) leads to the estimation of R_i . With this information, the signal can be reconstructed using (3).

Multiple channel consideration: Incorporating multiple measurement data has been introduced in [8]. Consider that the power system data has K channels which are obtained from the same period of time. For k -th channel ($k = 1, \dots, K$), the H matrix and Y vector can be formulated for every channel of the given data and notated as $H^{(k)}$ and $Y^{(k)}$. Then the a vector can be obtained by solving the following estimation problem.

$$\begin{aligned} & [(H^{(1)})^T \quad (H^{(2)})^T \quad \dots \quad (H^{(K)})^T]^T a \\ & = [(Y^{(1)})^T \quad (Y^{(2)})^T \quad \dots \quad (Y^{(K)})^T]^T \end{aligned} \quad (10)$$

B. Matrix Pencil

Consider a single measurement output, in MP, two shifted Hankel matrices H_1 and H_2 are used. A Hankel matrix is formed in (11). Deleting the last row results in H_1 while deleting the first row results in H_2 . Both matrices are of dimension $(L + 1) \times (N - L)$.

$$H = \begin{bmatrix} y_0 & y_1 & \cdots & y_{N-L-1} \\ y_1 & y_2 & \cdots & y_{N-L} \\ \vdots & \vdots & \ddots & \vdots \\ y_L & y_{L+1} & \cdots & y_{N-1} \\ y_{L+1} & y_{L+2} & \cdots & y_N \end{bmatrix}_{(L+2) \times (N-L)} \quad (11)$$

$$H_1 = H(1 : L + 1, :) \quad (12)$$

$$H_2 = H(2 : L + 2, :) \quad (13)$$

H_1 can be decomposed and expressed as follows.

$$H_1 = P \beta Q \quad (14)$$

where $P \in \mathbb{R}^{(L+1) \times n}$, $\beta \in \mathbb{R}^{n \times n}$, and $Q \in \mathbb{R}^{n \times (N-L)}$.

P , Q , and β are defined as follows.

$$P = \begin{bmatrix} 1 & 1 & \cdots & 1 \\ z_1 & z_2 & \cdots & z_n \\ \vdots & \vdots & & \vdots \\ z_1^L & z_2^L & \cdots & z_n^L \end{bmatrix}, Q = \begin{bmatrix} 1 & z_1 & \cdots & z_1^{N-L-1} \\ 1 & z_2 & \cdots & z_2^{N-L-1} \\ \vdots & \vdots & & \vdots \\ 1 & z_n & \cdots & z_n^{N-L-1} \end{bmatrix}, \quad (15)$$

$$\beta = \text{diag}([R_1, R_2, \cdots, R_n]).$$

H_2 can be expressed as:

$$H_2 = PZ_0\beta Q \quad (16)$$

where Z_0 is a diagonal matrix:

$$Z_0 = \text{diag}([z_1, z_2, \cdots, z_n]). \quad (17)$$

A generalized eigenvalue problem can be formulated based on the two shifted Hankel matrices. The eigenvalue z that can make $zH_1 - H_2$ to have a rank less than n must be one of the system eigenvalues z_i . This point can be proven by the following.

$$zH_1 - H_2 = zP\beta Q - PZ_0\beta Q = P(zI - Z_0)\beta Q. \quad (18)$$

Hence, if $z = z_i$, $zH_1 - H_2$ will have a rank less than n . Thus, z can be found by solving an ordinary eigenvalue problem:

$$zI - H_1^\dagger H_2. \quad (19)$$

Since H_1 and H_2 are Hankel matrices with rank n , SVD-based rank reduction can be performed on the two matrices. The rank reduction makes the eigenvalue identification robust against noise.

a) *SVD-based rank reduction*: SVD-based rank reduction is briefly described here. A thin matrix $A \in \mathbb{R}^{M \times N}$ with rank of N can be decomposed as the follows.

$$A = U_A S_A V_A^T \quad (20)$$

where $U_A \in \mathbb{R}^{M \times M}$ and $V_A \in \mathbb{R}^{N \times N}$ are two unitary matrices. $S_A \in \mathbb{R}^{M \times N}$ is a diagonal matrix with singular values of A ($\sigma_{A1} \geq \sigma_{A2} \cdots \geq \sigma_{AN} \geq 0$) as diagonal components. The rank reduction technique can be applied to (20) as follows.

$$A = [U_{A1} \quad U_{A2}] \begin{bmatrix} S_{A1} & 0 \\ 0 & S_{A2} \end{bmatrix} [V_{A1} \quad V_{A2}]^T \quad (21)$$

where $U_{A1} \in \mathbb{R}^{M \times n}$, $U_{A2} \in \mathbb{R}^{M \times (M-n)}$, $S_{A1} \in \mathbb{R}^{n \times n}$, $S_{A2} \in \mathbb{R}^{(M-n) \times (N-n)}$, $V_{A1} \in \mathbb{R}^{N \times n}$ and $V_{A2} \in \mathbb{R}^{N \times (N-n)}$. The reduced rank matrix A' is obtained as the following:

$$A \approx A' = U_{A1} S_{A1} V_{A1}^T \quad (22)$$

where A' has the same dimension of A . However, its rank is reduced to n .

SVD-based rank reduction can be applied to the Hankel matrix H in (11). The Hankel matrix is now expressed as follow.

$$H_{(L+2) \times (N-L)} = USV^T \quad (23)$$

where $U \in \mathbb{R}^{(L+2) \times n}$, $S \in \mathbb{R}^{n \times n}$, $V \in \mathbb{R}^{(N-L) \times n}$. The two shifted Hankel matrices can be expressed as follows.

$$H_1 = U_1 S V^T \quad (24)$$

$$H_2 = U_2 S V^T \quad (25)$$

where U_1 is the first $(L+1)$ rows of U and U_2 is the last $(L+1)$ rows of U .

Equation (18) can be expressed as follows.

$$zH_1 - H_2 = (zU_1 - U_2)S V^T. \quad (26)$$

Hence, z_i can be found as the eigenvalues of $U_1^\dagger U_2$.

b) *Multiple channel consideration*: Multiple channel handling technique is introduced in [21].

For each channel, two shifted Hankel matrices will be formed. Notate $H_1^{(k)}$ and $H_2^{(k)}$ as the Hankel matrices based on channel k . The aggregated Hankel matrices are as follows.

$$H_1 = [H_1^{(1)}, H_1^{(2)}, \cdots, H_1^{(K)}] \quad (27)$$

$$H_2 = [H_2^{(1)}, H_2^{(2)}, \cdots, H_2^{(K)}] \quad (28)$$

The two Hankel matrices can be decomposed in the similar aforementioned way.

$$H_1 = P\beta Q \quad (29)$$

$$H_2 = PZ_0\beta Q \quad (30)$$

where P and Z_0 are defined the same as those in (15) and (17). β and Q are defined as the aggregated ones. Consider $\beta^{(k)}$ and $Q^{(k)}$ as those formed based on k -th channel. Then the aggregated matrices are as follows.

$$\beta = [\beta^{(1)} \quad \beta^{(2)} \quad \dots \quad \beta^{(K)}] \quad (31)$$

$$Q = \text{diag}([Q^{(1)}, Q^{(2)}, \dots, Q^{(K)}]). \quad (32)$$

The system roots z_i can be obtained as the generalized eigenvalues that make the following matrix rank less than n :

$$zH_1 - H_2 \quad (33)$$

Similarly, SVD rank reduction can be applied to H_1 and H_2 . Based on those rank-reduced matrices, the eigenvalues will be found.

C. Eigensystem Realization Algorithm

Eigensystem realization algorithm (ERA) assumes that the dynamic response is due to an impulse input [6]. Consider a Linear-Time Invariant (LTI) system in discrete domain as the following:

$$x_{k+1} = Ax_k + Bu_k, y_k = Cx_k + Du_k \quad (34)$$

where $y \in \mathbb{R}^{K \times 1}$ is defined as the output column vector of the system with K output channels, $A \in \mathbb{R}^{n \times n}$, $B \in \mathbb{R}^{n \times 1}$, $C \in \mathbb{R}^{K \times n}$, and $D \in \mathbb{R}^{K \times 1}$ are system matrices. Assuming $x_0 = 0$, the system response due to an impulse input ($u_0 = 1$, $u_k = 0, k > 0$) can be found as follows.

$$\begin{aligned} x_0 &= 0, & y_0 &= D \\ x_1 &= B, & y_1 &= CB \\ x_2 &= AB, & y_2 &= CAB \\ &\dots & & \\ x_k &= A^{k-1}B, & y_k &= CA^{k-1}B \end{aligned} \quad (35)$$

Two shifted Hankel matrices are formed as follows.

$$\begin{aligned} H_1 &= \begin{bmatrix} y_1 & y_2 & \dots & y_L \\ y_2 & y_3 & \dots & y_{L+1} \\ \vdots & \vdots & \ddots & \vdots \\ y_{N-L+1} & y_{N-L+2} & \dots & y_N \end{bmatrix}_{K(N-L+1) \times L} \\ H_2 &= \begin{bmatrix} y_2 & y_3 & \dots & y_{L+1} \\ y_3 & y_4 & \dots & y_{L+2} \\ \vdots & \vdots & \ddots & \vdots \\ y_{N-L+2} & y_{N-L+3} & \dots & y_{N+1} \end{bmatrix}_{K(N-L+1) \times L} \end{aligned} \quad (36)$$

It can be seen that the Hankel matrices can be decomposed as follows.

$$H_1 = \begin{bmatrix} CB & CAB & \dots & CA^{L-1}B \\ CAB & CA^2B & \dots & CA^L B \\ \vdots & \vdots & \ddots & \vdots \\ CA^{N-L}B & CA^{N-L+1}B & \dots & CA^{N-1}B \end{bmatrix} \quad (37)$$

$$= \underbrace{\begin{bmatrix} C \\ CA \\ \vdots \\ CA^{N-L} \end{bmatrix}}_{\mathcal{O}} \underbrace{\begin{bmatrix} B & AB & \dots & A^{L-1}B \end{bmatrix}}_{\mathcal{C}} \quad (38)$$

$$H_2 = \mathcal{O}AC \quad (39)$$

where \mathcal{O} is the observability matrix and \mathcal{C} is the controllability matrix.

Note that the two matrices are of the following dimensions:

$$\begin{aligned}\mathcal{O} &\in \mathbb{R}^{K(N-L+1) \times n} \\ \mathcal{C} &\in \mathbb{R}^{n \times L}\end{aligned}$$

ERA employs SVD and further rank reduction to find two matrices to realize \mathcal{O} and \mathcal{C} . First, SVD is conducted for H_1 and the resulting matrices are marked with their dimensions as follows.

$$\begin{aligned}H_1 &= USV^T, \\ \text{where } U &\in \mathbb{R}^{K(N-L+1) \times K(N-L+1)}, \\ S &\in \mathbb{R}^{K(N-L+1) \times L}, \quad V \in \mathbb{R}^{L \times L}\end{aligned}\tag{40}$$

Only n components of $\text{diag}(S)$ will be kept to construct the reduced-rank Hankel matrix H'_1 .

$$\begin{aligned}H'_1 &= \underbrace{U(:, 1:n)}_{U'} \underbrace{S(1:n, 1:n)}_{S'} \underbrace{(V(:, 1:n))^T}_{V'} \\ U' &\in \mathbb{R}^{K(N-L+1) \times n}, \\ S' &\in \mathbb{R}^{n \times n}, \quad V' \in \mathbb{R}^{L \times n}\end{aligned}\tag{41}$$

Similarly, rank reduction may also be applied to H_2 to have a low-rank Hankel matrix H'_2 . It is worth to mention that this step on H_2 rank reduction is not used in [6]. Rank reduction for H_2 leads to a superior performance as demonstrated in the case studies in Section IV. From the reduced-rank Hankel matrix, the observability and controllability matrices can be realized as follows.

$$\mathcal{O} = U' S'^{\frac{1}{2}}, \quad \mathcal{C} = S'^{\frac{1}{2}} (V')^T\tag{42}$$

Thus, the system matrix A can be realized through the use of (39).

$$A = S'^{-\frac{1}{2}} U'^T H'_2 V' S'^{-\frac{1}{2}}\tag{43}$$

From A , eigenvalues of the discrete system can be found.

III. ORDER REDUCTION TECHNIQUES

The objective is to obtain eigenvalues of a low-order system. SVD rank reduction has been employed in MP and the order of the system can be specified. Performance of MP is excellent in terms of noise handling. One reason is that SVD-based reduction rules out many small singular values which are related to noise. With this procedure, MP is shown to have a better performance over Prony analysis [11]. This point is also validated for power system oscillation studies in [13].

In this section, SVD rank reduction technique is explored to improve the performance of Prony analysis.

In [11], Hankel matrix rank reduction is suggested for Prony analysis to better handle noise. On the other hand, the dimension of the Hankel matrix is the same even if the rank reduction was applied. In the following, an RLC circuit example is presented to first illustrate the effect on eigenvalue distribution with Hankel matrix rank reduction. As a consequence of rank reduction, distribution of eigenvalues has a radical change. The dominant eigenvalues and the non-dominant eigenvalues become clearly separated. With this effect, the non-dominant eigenvalues are further eliminated. Thus, a low-order system is identified. Similar improvement for Prony analysis has been presented in [20]. However, the effect of rank reduction on eigenvalue distribution is not demonstrated.

A series RLC circuit shown in Fig. 1 is used as an illustrative example. A step change in the source voltage is applied at $t = 0$ second, the current and the capacitor voltage are chosen as the measurement. The current i and voltage V_c in Laplace domain are expressed as follows.

$$\begin{aligned}i &= \frac{C}{LCs^2 + RCs + 1} \\ V_c &= \frac{1}{s(LCs^2 + RCs + 1)}\end{aligned}\tag{44}$$

Obviously, the two signals have different number of eigenvalues. The current has two poles: $\lambda \approx -\frac{R}{2L} \pm j\frac{1}{\sqrt{LC}}$. The voltage has these two poles and an additional pole as 0.

The sampling rate is 0.001 s for the measurement data. The number of samples in 0.1 seconds is 101 ($N = 101$). The system is assumed to have an order of 33. As a result, the Hankel matrix dimension is 68×33 . As a comparison, order 3 is assumed for another case. The resulting Hankel matrix has a dimension of 98×3 . For each order assumption, signals with and without noise (0.3 pu uniformly distributed) are examined. Fig. 2 presents the two cases when order is assumed as 33, and Fig. 3 presents the two cases when the order is assumed as 3.

It can be seen that when the signals have no noise pollution, Prony analysis with different order assumptions correctly reflects the eigenvalues (Figs. 2a and 3a). The reconstructed signals match the original signals well. From Fig. 2a, it can also be observed that if the Hankel matrix has a low rank, the resulting identified eigenvalues distribute on the real and imaginary space with an obvious pattern. The system modes $(0, -37.7 \pm 2\pi 37.47)$ are clearly separated from the other modes.

When the signals are polluted with noise (Figs. 2b and 3b), it can be seen that the reconstructed signals match the original ones well when the order is assumed high. If a low order is assumed, the match is poor. In addition, the identified eigenvalues for the 33 order system no longer have a clear pattern when there is noise. The 37 Hz LC resonance mode is located more towards the left half-plane (LHP) compared to several other modes.

Rank reduction on the Hankel matrix has a significant effect. Using the same noise polluted signals shown in Fig. 2b and applying rank reduction on the corresponding 68×33 Hankel matrix, the resulting rank-3 Hankel matrix leads to system eigenvalues (shown in Fig. 4a) with a similar pattern as that shown in Fig. 2a. The three dominant eigenvalues are clearly separated from the rest. As a step further, only the three dominant eigenvalues are kept. The reconstructed signals are shown in Fig. 4b. It can be seen that the reconstructed signals are substantially smoother compared to those in Fig. 4a.

Remarks: A reduced-order Prony analysis has been developed using Hankel matrix rank reduction and eigenvalue reduction techniques. The improved Prony analysis shows that it can correctly identify the system poles from noisy signals.

IV. MORE CASE STUDIES

Three more case studies are presented in this section, namely, large-scale power grid oscillations, SSR in type-3 wind generator interconnected with series compensated networks, and real-world oscillation events. All of the proposed methods and simulations are implemented in MATLAB. The measurement data for the 16-machine 68-bus system are generated using the power system toolbox (PST) [22], which is a MATLAB-based power system dynamic simulation. The measurement data for the type-3 wind SSR and the real-world oscillation events are generated using a MATLAB/SimPowerSystems testbed and MATLAB, respectively.

A. Power Grid Oscillations

The 16-machine 68-bus test case system (shown in Fig. 5) is used for eigenvalue estimation of large-scale power grid oscillations. This system represents the New England Test System (NETS)-New York Power System (NYPS) interconnected system [23] and has five areas. NETS is represented by area 4 which has generators G1 to G9, while NYPS is represented by area 5 which has generators G10 to G13. Three other areas have equivalent generators G14 to G16.

Simulation results are produced by power system toolbox (PST) [22]. The dynamic event applied is a three-phase fault on line 29-28 at Bus 28 side. It is cleared in 0.01 seconds and the line is tripped after another 0.05 seconds. Dynamic simulation data after the line tripping are used for eigenvalue estimation.

The network assumes algebraic voltage and current relationship, while the 16 machines are modeled as second-order system. Small signal analysis of PST gives 32 eigenvalues. Among them, four pairs of complex conjugate eigenvalues correspond to inter-area oscillation modes with frequency in the range of 0.3 Hz to 0.8 Hz.

In this case study, eigenvalues from a reduced-order system are sought based on measurements. First, the system is assumed to have an order of 10 as this five-area system is known to be represented by five equivalent generators, each of two orders [3].

Two voltage deviation signals in different areas (Bus 5 in Area 4 and Bus 67 in Area 1) are chosen for eigenvalue estimation and signal reconstruction. Those two signals are re-sampled with sampling time interval of 0.02 s. Further, Bus 67's signal is scaled up 100 times to be in the same order as that from Bus 5. The time periods for all tests are 10 seconds.

Traditional Prony analysis without rank reduction cannot give adequate reconstructed signals even with high orders. Therefore, the proposed reduced-order Prony analysis is applied. The number of samples is $N = 486$ for each measurement data. The Hankel matrix width for the rank reduced Prony analysis is set to be 250. The L parameter for MP and ERA is chosen as 180. Reduced-order Prony analysis can provide accurate reconstructed signals as MP and ERA, shown in Fig. 6a. The estimated eigenvalues of the three methods are shown in Fig. 6b. It can be seen that all three methods give accurate signal matching results. In addition, seven eigenvalues, including one at the origin, three modes at 0.37 Hz, 0.6 Hz, and 0.78 Hz, are identified by all three methods.

Further order reduction is applied to test the capability of each method. The number of the order is reduced to be 4.

Fig. 7 presents the estimation results when the order is assumed as 4. It can be seen that ERA and reduced-order Prony lead to good signal matching results. Two inter-area oscillation modes are identified by these two methods. On the other hand, MP does not give good signal matching results. MP identifies one mode in the inter-area oscillation frequency range, and two real eigenvalues with one at the origin and another further left.

Remarks: The three methods can all give reduced-order eigenvalues for power grid oscillation case study. Reduced-order Prony and ERA show stronger capability in handling reduced-order systems compared to MP.

B. Type-3 Wind SSR

While the previous case study is related to large-scale power grid on low-frequency oscillation, this case study is on type-3 wind SSR dynamics. This type of phenomena appears when large wind farms are integrated into series compensated network [24]. The SSR is related to the LC resonant mode, induction generator effect, and converter controllers [25]. Frequency of SSR ranges from several Hz to nominal frequency.

A testbed of a type-3 wind interconnected with a series compensated network is shown in Fig. 8.

A 1.5 MW DFIG wind turbine is connected to a 50 Hz system through two parallel lines. One line has series compensation. The compensation level of the line is 10%. At $t = 5$ s, the line without series compensation is tripped. The compensation level of the entire system, considering the transformer reactance X_{T1} and the wind turbine leakage reactance, is approximately 4%. This will result in SSR of 0.2 pu frequency or 10 Hz in the abc frame. For variables with constant values at steady-state, e.g., magnitudes of voltage or current and power, the oscillation frequency will be 50 Hz. Fast Fourier Transformation (FFT) analysis shows that the oscillation indeed has a frequency of 10 Hz in abc voltages and currents. In real power, the oscillation frequency is 50 Hz.

The simulation is carried out in MATLAB/SimPowerSystems. Fig. 9a shows the simulation results of grid currents I_{B120} , line currents I_{Bg} , rotor-side converter (RSC) currents I_{rsc} , and grid-side converter (GSC) currents I_{gsc} . Fig. 9b gives the phase A current from the grid, its FFT plots, real power from the wind P and its FFT plots. It can be seen that 10 Hz oscillations appear in the current, while 50 Hz oscillations appear in the power.

The real power and reactive power measurements from 5 seconds to 5.15 seconds are analyzed for eigenvalue estimation. The sampling rate is 50 μ s. The number of samples taken is 3001. For matrix Pencil and ERA, the parameter L related to Hankel matrix formulation is chosen to be 1000. The Hankel matrix width of rank reduced Prony analysis is 2200.

The simulation testbed includes electromagnetic dynamics of line and grid, induction generators, RSC controls, GSC controls, GSC converter filters, phase-locked loop, dc-link capacitor as well as wind turbine mechanical dynamics. The order of the dynamic system is approximately 30.

Two orders are tested for reduced-order system eigenvalue estimation: 10 and 4. Fig. 10a presents the reconstructed signals and the estimated eigenvalues when the order is assumed as 10. Fig. 10b presents the reconstructed signals and the estimated eigenvalues when the order is assumed as 4.

It can be observed that all three methods can give an accurate identification of the dominant mode at 50 Hz. When the order assumption is 10, MP and ERA give a slightly better signal matching for real power. When the order assumption is 4, all three methods give similar signal matching results. While the 50 Hz dominant eigenvalues are identified by all three methods, MP and ERA show an additional pair of complex conjugate eigenvalues located close to the origin. On the other hand, reduced-order Prony analysis shows two real eigenvalues with one at the origin and the other further left.

Remarks: Dominant eigenvalues can be identified with accuracy. All three methods give similar performance in identifying eigenvalues of reduced-order systems.

C. Real-World Oscillation Events

In order to validate the effectiveness of the proposed methods, real-world oscillation events are analyzed. A test cases library of power system oscillations is presented in [26], and the real-world oscillation data can be found in [27]. The oscillation events are captured by Independent System Operator-New England (ISO-NE), which is a part of the eastern interconnection in the United States. PMU measurements are collected from different locations of the ISO-NE system during the oscillatory events. Two oscillation events are investigated and analyzed in this paper. The simulation results are carried out in MATLAB.

c) Oscillation Event 1 : Oscillation Event 1 occurred in June 17, 2016 with a dominant mode of 0.27 Hz due to an issue of a generator in the southern area of the eastern interconnection which is out of the ISO-NE area [27]. The PMU measurements are provided for the first 3 minutes of this oscillation event. Phase-to-ground voltage magnitudes are shown in Fig. 11a. Two voltage signals from different substations are selected: Signal 5 (Substation 2) and Signal 13 (Substation 5). The voltage measurements from 40 to 60 seconds are analyzed to detect the inter-area oscillation. The sampling rate is 0.034 seconds, and the number of samples is 601. The Hankel matrix width of the reduced-order Prony analysis is 280, while L parameter for ERA and MP is 200.

First, the system order is assumed as 15 to test the ability of the three methods to identify the inter-area oscillation. All of the three methods can provide accurate reconstructed signals compared to the original measurements as shown in Fig. 12a. The estimated eigenvalues are presented in Fig. 12b. It can be seen that the three methods can identify the oscillation mode of 0.27 Hz. The proposed Prony analysis has the dominant mode on the right half-plane (RHP), and the refined ERA has the dominant mode far right compared to the other modes. On the other hand, MP has three additional pair of complex conjugate eigenvalues on the RHP along with the dominant mode. This gives an advantage to the proposed Prony analysis and ERA which can clearly detect the inter-area oscillation mode.

In addition, the system order is reduced to be 3 to investigate the effect of the order assumptions. Fig. 13 presents the reconstructed signals and the estimated eigenvalues of the three methods when the order is assumed as 3. It can be observed that the three methods have adequate reconstructed signals compared to the original signals. Also, all of the three methods can identify the dominant mode of 0.27 Hz.

d) Oscillation Event 2: Oscillation Event 2 occurred in October 3, 2017 due to an issue of a generator governor outside of the ISO-NE, and it has three dominant modes of 0.08, 0.15, and 0.31 Hz [27]. Six minutes of this oscillatory event are provided from PMU data. Those PMU measurements contain some bad data which should be removed to get the correct signals. Fig. 11b presents the phase-to-ground voltage magnitude of this event. To identify the inter-area modes, the voltage measurements from 270 to 300 seconds are analyzed, and all of the signals are considered in this case. The number of samples is 901, and the sampling rate is 0.034 seconds. The Hankel matrix width of the three methods is 400.

To examine the capability of each method, the system order is assumed as 15. All of the three methods have accurate reconstructed signals as shown in Fig. 14a. The estimated eigenvalues of this case are shown in Fig. 14b. It can be seen that the proposed Prony analysis and ERA clearly have the three dominant modes on the RHP. In contrast, MP has two dominant modes (0.15 and 0.31 Hz) on the RHP and one mode of 0.08 Hz on the LHP which can be challenging to identify the dominant modes for this method. It should be noted that the three methods have one additional pair of complex conjugate eigenvalues on the RHP. Lower orders such as 3 or 4 cannot provide accurate reconstructed signals and may not detect some of the inter-area oscillations of Event 2. Note that order 15 is the lowest order that can obtain well-matched reconstructed signals in this case.

Remarks: The dominant modes of the real-world oscillation events can be identified with accuracy. Reduced-order Prony analysis and ERA have a superior performance in identifying the dominant modes compared to MP.

D. Development Discussion and Future Research

The three measurement-based identification methods are investigated in this paper. Prony analysis method is improved to achieve reduced-order system eigenvalue identification and noise resilience. Traditional Prony analysis cannot obtain adequate reconstructed signals and detect the inter-area oscillations with low order assumptions especially in the case of noisy signals as discussed in Section III. Fig. 15 presents a comparison of the traditional and proposed Prony analysis using the 16-machine 68-bus test case system with assumed order of 10. It can be seen that the proposed Prony analysis has a better signal reconstruction and eigenvalue estimation compared to the traditional method. When the order is assumed as 4, traditional Prony analysis is not able to obtain a proper result. It also cannot work out the type-3 wind SSR system and the real-world oscillation events with low order assumptions.

In addition, traditional ERA Hankel matrices are improved to handle multi-channel data, and the rank reduction technique is applied to the second shifted Hankel matrix of ERA to enhance its performance. A comparison between the traditional and proposed ERA on the 68-bus system is presented in Fig. 16 considering one signal (Bus 67) since the traditional method cannot handle more than one signal. It can be observed that the proposed ERA has a better signal matching and eigenvalue estimation compared to the traditional one. Also, it should be noted that the proposed ERA can obtain a better eigenvalue distribution when more than one signal is analyzed. Traditional ERA is not able to identify the dominant modes of the type-3 wind SSR system and the real-world oscillation events with low orders.

Hence, the reduced-order Prony analysis and refined ERA have a better performance in detecting the inter-area oscillation modes and providing the reconstructed signals compared to the traditional approaches.

Different order assumptions are tested and investigated in this paper. The chosen order should be low to adequately identify the dominant modes. The best order assumption is the lowest order that can provide accurate reconstructed signals. This lowest order can clearly detect the inter-area oscillation modes. Order assumptions from 3 to 20 are most effective orders with different systems and PMU measurements, and the lowest one which can provide well-matched signals should be chosen.

The computational time of the three methods is compared as shown in Table I. The three methods have similar CPU time when the number of samples are not large, while MP has a better CPU time compared to reduced-order Prony analysis and ERA in the case of the large number of samples. Although MP is faster in this case, the proposed Prony analysis and ERA have a superior result. It can also be seen that the reduced-order Prony analysis and MP are faster compared to ERA when the number of analyzed signals is large.

Prony analysis, MP, and ERA have proven their capabilities to identify the inter-area oscillation modes in different power system applications including real-world oscillatory events. The methods may lead to future research on constructing reduced-order dynamic system models. For example, ERA method can reveal the system dynamic matrix with a certain order as well as dominant modes, without prior information of the system. Thus, a dynamic system with this order can be constructed with structures known and parameters to be tuned. Optimization methods may be employed to tune these parameters to have the eigenvalues of the reduced-order dynamic system locating as close as possible to the identified eigenvalues. With this research, generator parameters such as inertia constant, damping coefficients, and regulation speed constant can be estimated.

V. CONCLUSION

This paper examines the principles, multi-channel data handling, noise resilience techniques of three eigenvalue identification methods used in power systems: Prony analysis, Matrix Pencil (MP), and Eigensystem Realization Algorithm (ERA). SVD-based rank reduction technique is identified as the key to noise resilience and order reduction. Accordingly, ERA method is refined by applying SVD-based rank reduction on both Hankel matrices. A reduced-order Prony analysis method through Hankel matrix rank reduction is invented. The new Prony analysis can accurately identify system eigenvalues from noisy

signals. Four case studies are presented to illustrate the three methods, including a tutorial example on RLC circuit resonance, a large-scale power grid oscillation example, a type-3 wind SSR example, and real-world oscillation events. The case study results demonstrate the efficacy of all three methods in accurate eigenvalue identification.

REFERENCES

- [1] S. Brahma, R. Kavasseri, H. Cao, N. Chaudhuri, T. Alexopoulos, and Y. Cui, "Real-time identification of dynamic events in power systems using pmu data, and potential applications, models, promises, and challenges," *IEEE transactions on Power Delivery*, vol. 32, no. 1, pp. 294–301, 2017.
- [2] H. R. Ali, L. P. Kunjumammed, B. C. Pal, A. Adamczyk, and K. Vershinin, "Model order reduction of wind farms: Linear approach," *IEEE Transactions on Sustainable Energy*, 2018.
- [3] J. H. Chow, *Power system coherency and model reduction*. Springer, 2013.
- [4] J. Turunen, J. Thambirajah, M. Larsson, B. C. Pal, N. F. Thornhill, L. C. Haarla, W. W. Hung, A. M. Carter, and T. Rauhala, "Comparison of three electromechanical oscillation damping estimation methods," *IEEE Transactions on power systems*, vol. 26, no. 4, pp. 2398–2407, 2011.
- [5] J. K. Hwang and Y. Liu, "Identification of interarea modes from ringdown data by curve-fitting in the frequency domain," *IEEE Transactions on Power Systems*, vol. 32, no. 2, pp. 842–851, 2017.
- [6] M. Crow, M. Gibbard, A. Messina, J. Pierre, J. Sanchez-Gasca, D. Trudnowski, and D. Vowles, "Identification of electromechanical modes in power systems," *IEEE Task Force Report, Special Publication TP462*, 2012.
- [7] J. F. Hauer, C. Demeure, and L. Scharf, "Initial results in prony analysis of power system response signals," *IEEE Transactions on power systems*, vol. 5, no. 1, pp. 80–89, 1990.
- [8] D. Trudnowski, J. Johnson, and J. Hauer, "Making prony analysis more accurate using multiple signals," *Power Systems, IEEE Transactions on*, vol. 14, no. 1, pp. 226–231, 1999.
- [9] L. Fan, "Data fusion-based distributed prony analysis," *Electric Power Systems Research*, vol. 143, pp. 634–642, 2017.
- [10] Y. Hua and T. K. Sarkar, "Matrix pencil method for estimating parameters of exponentially damped/undamped sinusoids in noise," *IEEE Transactions on Acoustics, Speech, and Signal Processing*, vol. 38, no. 5, pp. 814–824, 1990.
- [11] T. K. Sarkar and O. Pereira, "Using the matrix pencil method to estimate the parameters of a sum of complex exponentials," *IEEE Antennas and Propagation Magazine*, vol. 37, no. 1, pp. 48–55, 1995.
- [12] M. L. Crow and A. Singh, "The matrix pencil for power system modal extraction," *IEEE Transactions on Power Systems*, vol. 20, no. 1, pp. 501–502, 2005.
- [13] L. L. Grant and M. L. Crow, "Comparison of matrix pencil and prony methods for power system modal analysis of noisy signals," in *North American Power Symposium (NAPS), 2011*. IEEE, 2011, pp. 1–7.
- [14] J.-N. Juang and R. S. Pappa, "An eigensystem realization algorithm for modal parameter identification and model reduction," *Journal of guidance, control, and dynamics*, vol. 8, no. 5, pp. 620–627, 1985.
- [15] E. G. Gilbert, "Controllability and observability in multivariable control systems," *Journal of the Society for Industrial and Applied Mathematics, Series A: Control*, vol. 1, no. 2, pp. 128–151, 1963.
- [16] R. E. Kalman, "Mathematical description of linear dynamical systems," *Journal of the Society for Industrial and Applied Mathematics, Series A: Control*, vol. 1, no. 2, pp. 152–192, 1963.
- [17] J. Sanchez-Gasca and J. Chow, "Computation of power system low-order models from time domain simulations using a hankel matrix," *IEEE Transactions on Power Systems*, vol. 12, no. 4, pp. 1461–1467, 1997.
- [18] E. Barocio, B. C. Pal, N. F. Thornhill, and A. R. Messina, "A dynamic mode decomposition framework for global power system oscillation analysis," *IEEE Transactions on Power Systems*, vol. 30, no. 6, pp. 2902–2912, 2015.
- [19] Y. Hua and T. K. Sarkar, "On svd for estimating generalized eigenvalues of singular matrix pencil in noise," in *1991., IEEE International Symposium on Circuits and Systems*. IEEE, 1991, pp. 2780–2783.
- [20] J. Xiao, X. Xie, Y. Han, and J. Wu, "Dynamic tracking of low-frequency oscillations with improved prony method in wide-area measurement system," in *IEEE Power Engineering Society General Meeting, 2004*. IEEE, 2004, pp. 1104–1109.
- [21] T. K. Sarkar, S. Park, J. Koh, and S. M. Rao, "Application of the matrix pencil method for estimating the sem (singularity expansion method) poles of source-free transient responses from multiple look directions," *IEEE Transactions on Antennas and Propagation*, vol. 48, no. 4, pp. 612–618, 2000.
- [22] J. H. Chow and K. W. Cheung, "A toolbox for power system dynamics and control engineering education and research," *IEEE transactions on Power Systems*, vol. 7, no. 4, pp. 1559–1564, 1992.
- [23] G. Rogers, *Power system oscillations*. Springer Science & Business Media, 2012.
- [24] G. D. Irwin, A. K. Jindal, and A. L. Isaacs, "Sub-synchronous control interactions between type 3 wind turbines and series compensated ac transmission systems," in *2011 IEEE power and energy society general meeting*. IEEE, 2011, pp. 1–6.

- [25] L. Fan, R. Kavasseri, Z. L. Miao, and C. Zhu, "Modeling of dfig-based wind farms for ssr analysis," *IEEE Transactions on Power Delivery*, vol. 25, no. 4, pp. 2073–2082, 2010.
- [26] S. Maslennikov, B. Wang, Q. Zhang, E. Litvinov *et al.*, "A test cases library for methods locating the sources of sustained oscillations," in *2016 IEEE Power and Energy Society General Meeting (PESGM)*. IEEE, 2016, pp. 1–5.
- [27] Test cases library of power system sustained oscillations. [Online]. Available: <http://web.eecs.utk.edu/~kaisun/Oscillation/>

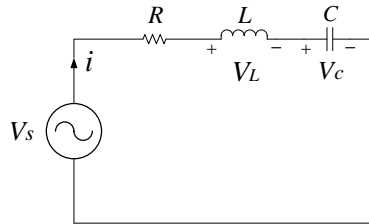


Fig. 1: RLC circuit.

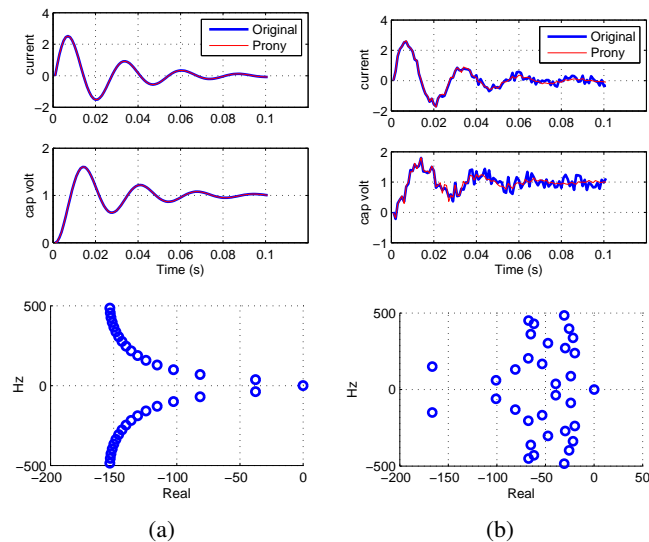


Fig. 2: RLC circuit reconstructed signals and estimated eigenvalues with assumed order of 33. (2a) without noise. (2b) with noise.

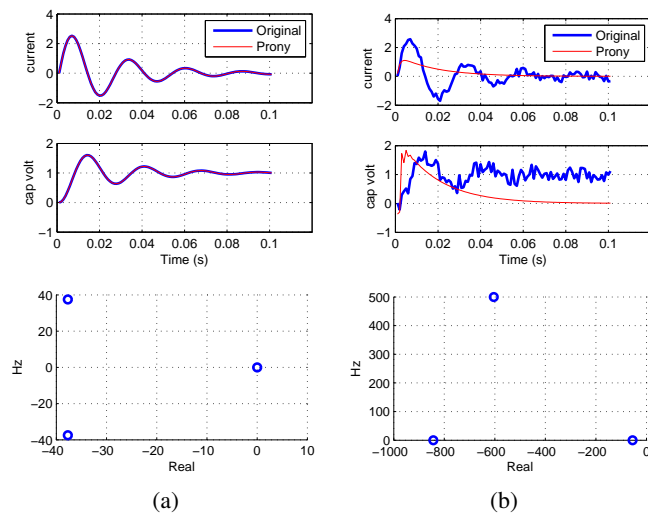


Fig. 3: RLC circuit reconstructed signals and estimated eigenvalues with assumed order of 3. (3a) without noise. (3b) with noise.

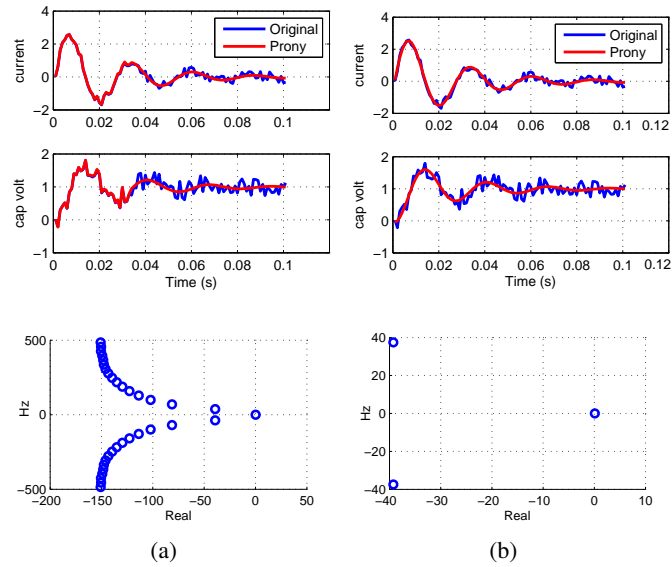


Fig. 4: Reduced-order Prony analysis results of the RLC circuit. (4a) with Hankel matrix rank reduction. (4b) with rank reduction and eigenvalue reduction techniques.

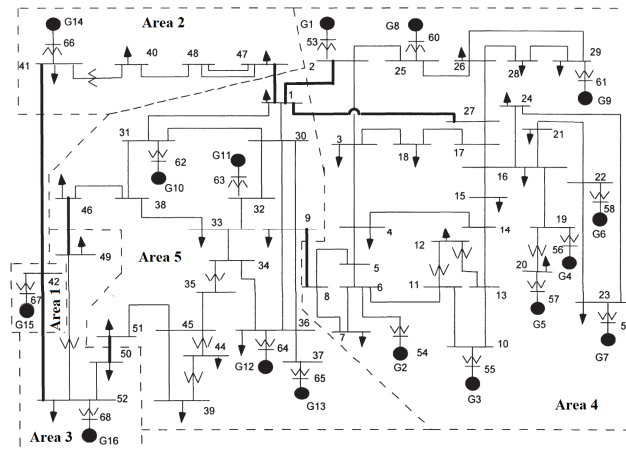


Fig. 5: 16-machine 68-bus test case system [23].

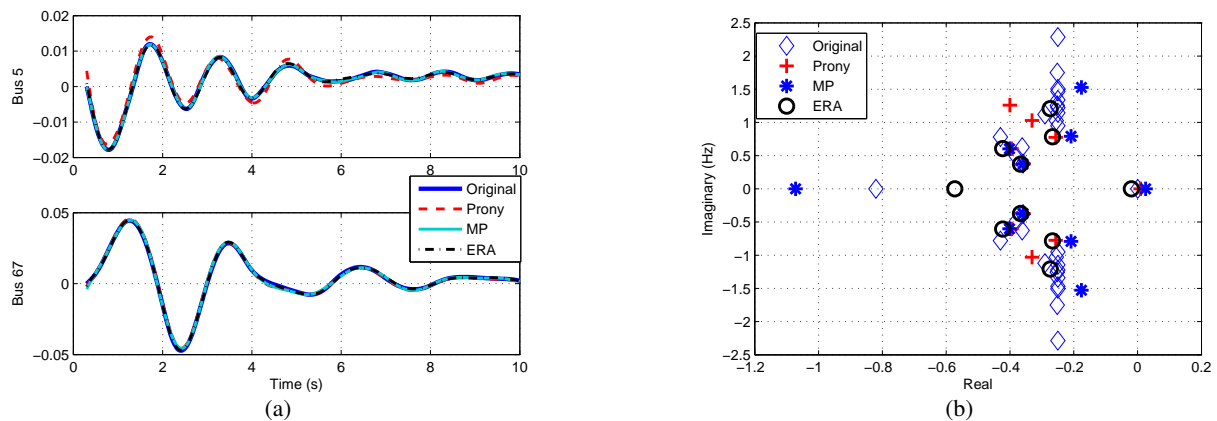


Fig. 6: Large-scale power grid oscillation signal reconstruction and eigenvalue estimation. Order is 10.

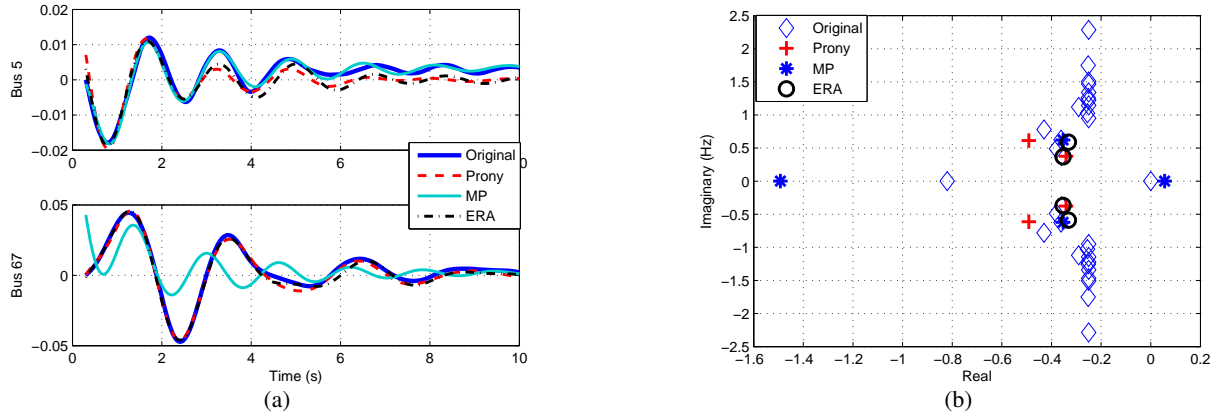


Fig. 7: Large-scale power grid oscillation signal reconstruction and eigenvalue estimation. Order is 4.

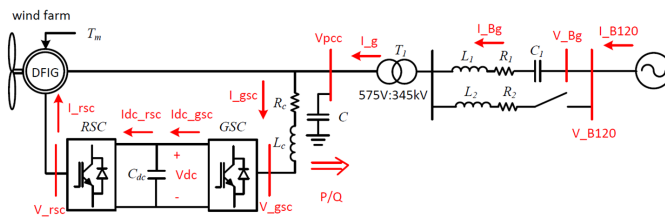


Fig. 8: Type 3 wind generator SSR testbed.

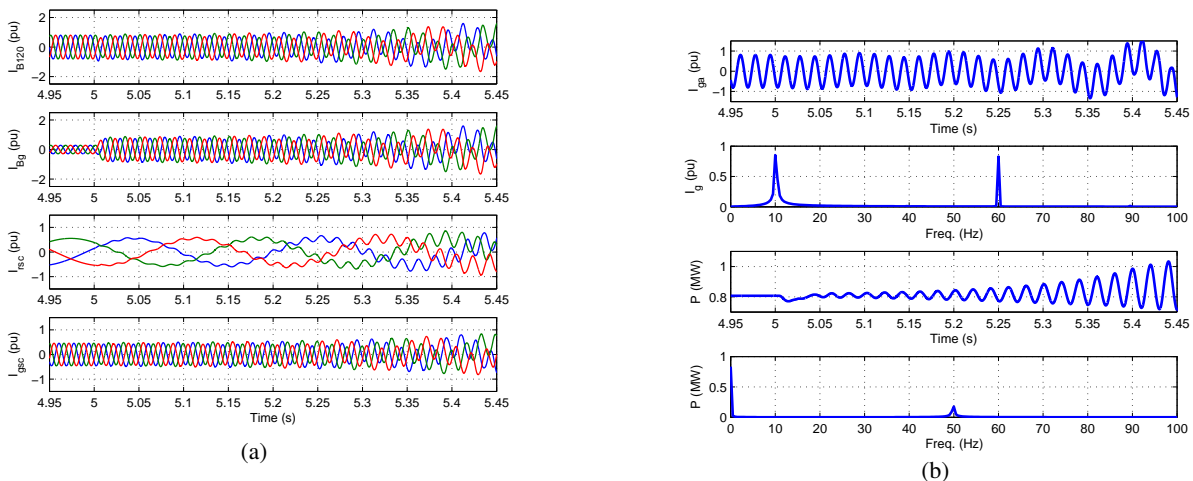


Fig. 9: Simulation results. (9a) Currents: grid, line, RSC and GSC. (9b) Grid current FFT and real power FFT.

TABLE I. CPU TIME COMPARISON OF THE THREE METHODS

System	Number of Samples	Number of Signals	Simulation Time (s)	CPU Time (s)		
				Prony	ERA	MP
NETS-NYPS	486	2	10	0.4531	0.4688	0.4063
Type-3 Wind SSR	3001	2	10	62.0156	62.8281	6.1875
ISO-NE (Event 1)	601	2	20	0.5625	0.5625	0.4375
ISO-NE (Event 2)	901	25	30	18.7188	47.2031	18.2969

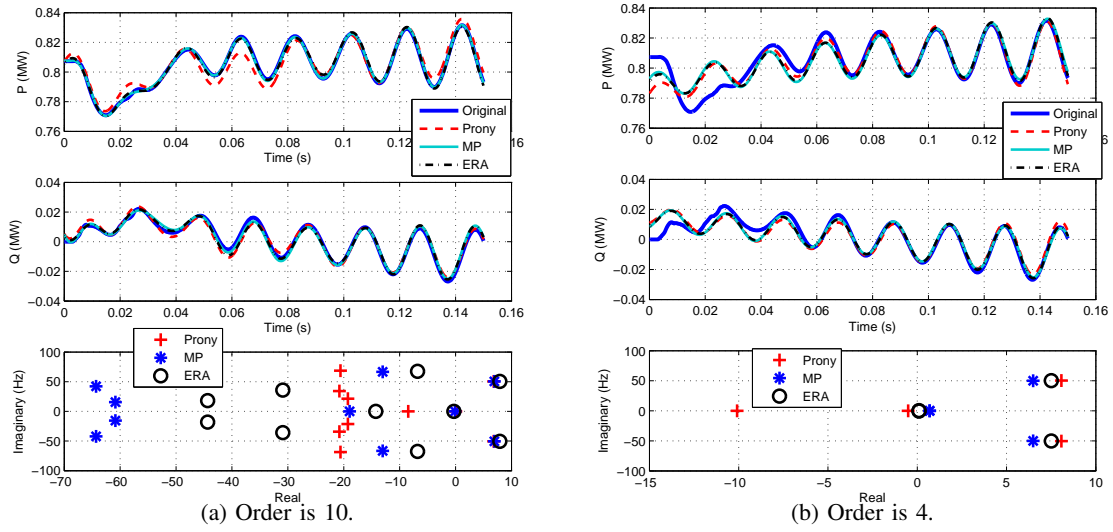


Fig. 10: Comparison of reconstructed signals and the estimated eigenvalues.

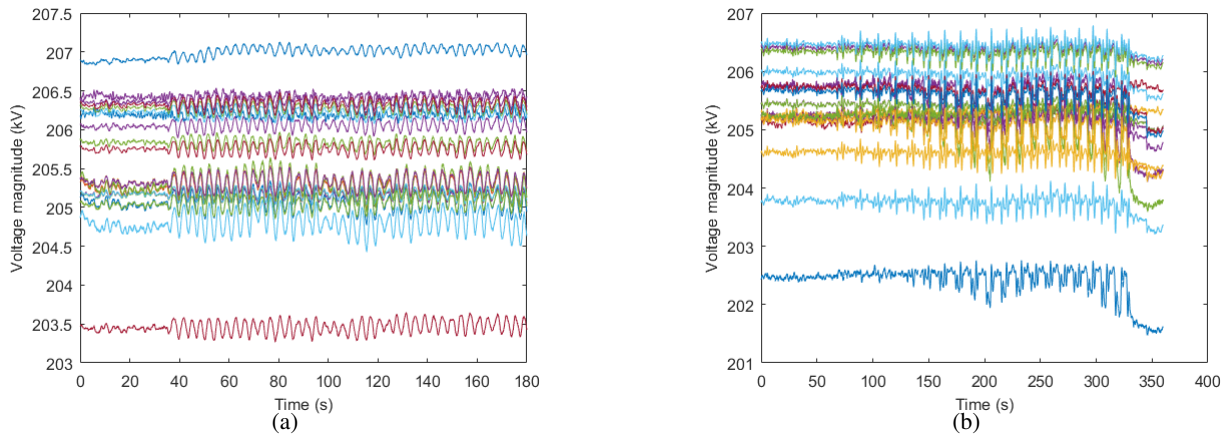


Fig. 11: Phase-to-ground voltage magnitudes during the oscillatory events. (11a) Event 1. (11b) Event 2.

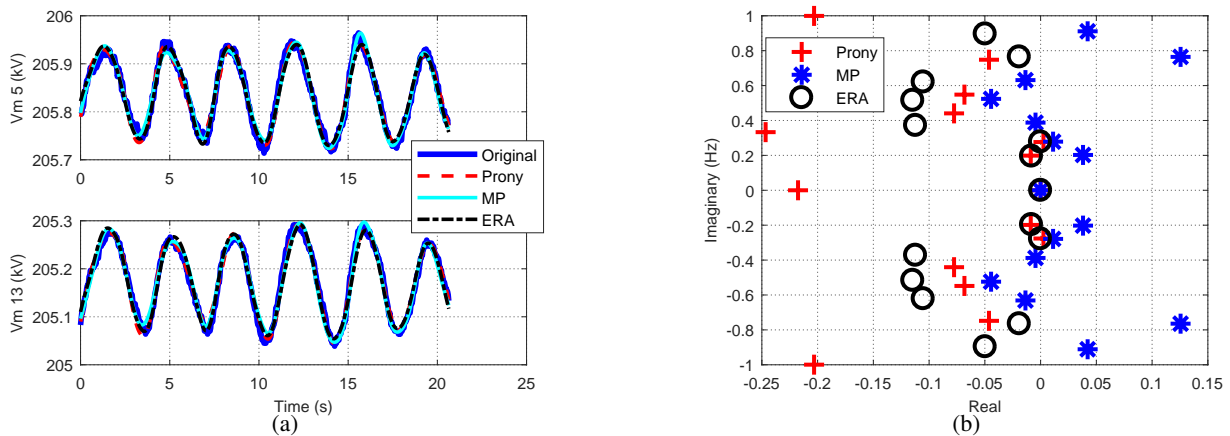


Fig. 12: Signal reconstruction and eigenvalue estimation of Event 1 with assumed order of 15.

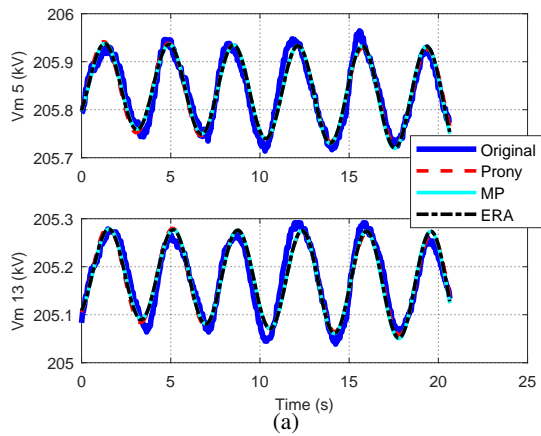


Fig. 13: Signal reconstruction and eigenvalue estimation of Event 1 with assumed order of 3.

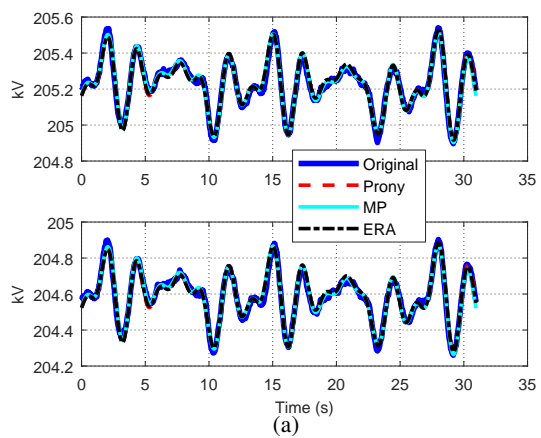


Fig. 14: Event 2 signal reconstruction and eigenvalue estimation.

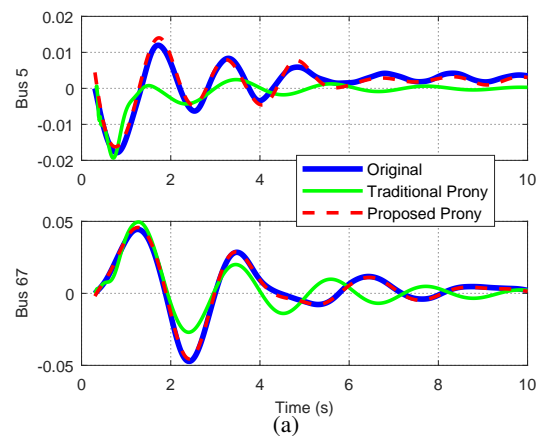


Fig. 15: Comparison of traditional and proposed Prony analysis on the 68-bus system.

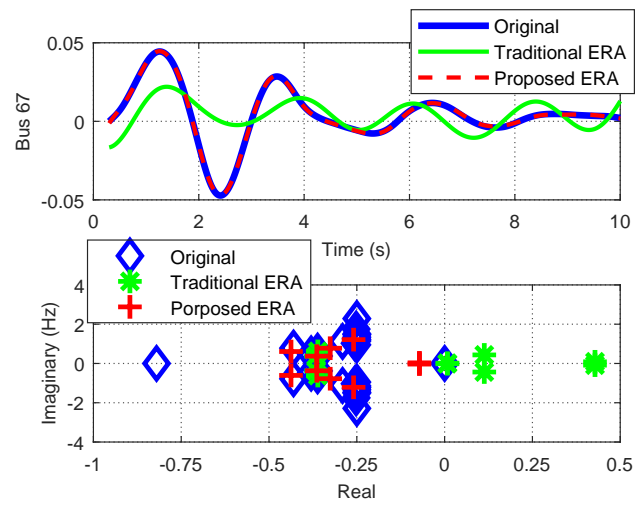


Fig. 16: Comparison of traditional and proposed ERA on the 68-bus system.